Analysis of Laser and Detector Placement in MIMO Multimode Optical Fiber Systems

Kumar Appaiah, Sagi Zisman, Sriram Vishwanath, Seth R. Bank
Department of Electrical and Computer Engineering
The University of Texas at Austin
Austin, TX - 78712
Email: {kumar.a,sagi.zisman}@utexas.edu

***Abstract*—Multimode fibers (MMFs) offer a cost-effective connection solution for small and medium length networks. However, data rates through multimode fibers are traditionally limited by modal dispersion. Signal processing and Multiple-Input Multiple-Output (MIMO) have been shown to be effective at combating these limitations, but device design for the specific purpose of MIMO in MMFs is still an open issue. This paper utilizes a statistical field propagation model for MMFs to aid the analysis and designs of MMF laser and detector arrays, and aims to improve data rates of the fiber. Simulations reveal that optimal device designs could possess 2-3 times the data carrying capacity of suboptimal ones.**

I. Introduction

Optical fibers form an integral part of current networking architectures owing to their ability to support extremely high data rates. In recent times, single-mode fibers (SMFs) have displaced multimode fibers (MMFs) as the choice for high-speed and long-distance optical links owing to their low dispersion and high data carrying abilities. However, these improvements also come with additional complexity in alignment and packaging, thus making them costly and unattractive for small and medium sized networks. On the other hand, MMFs are hampered by greater modal dispersion. Several recent advances in dispersion compensation techniques have improved data rates through multimode fibers [1, 2]. However, to offer even greater speeds, it is essential to utilize the fundamental propagation characteristics of MMFs, which is the goal of techniques such as mode-division multiplexing and multiple-input multiple-output (MIMO). While earlier work has shown the usefulness of MIMO techniques in MMFs [3–6], a fundamental analytical framework for MIMO communication over MMFs is yet absent. The goal of this paper is to develop such a framework, and by doing so, enable device design to maximize the benefits of MIMO and signal processing techniques for MMFs.

The primary motivation for this work stems from antenna placement concepts in wireless MIMO systems [7]. In wireless MIMO systems, carefully designed antenna placement ensures the independence of channel coefficients, which enhances the channel's diversity and multiplexing capabilities. An analogous problem in the MMF-MIMO context would be to determine the optimal placement strategies for lasers and detectors. To this end, we adopt the field propagation analysis technique developed by Shemirani et al. [8] and apply it to the MIMO-MMF channel to study the role of laser and detector placement on channel performance. We determine placement strategies with the intent of maximizing the information theoretic capacity. Our results show that optimal placement strategies yield 2-3 times the capacities of arbitrary placements due to improved modal diversity.

In recent years, MIMO and signal processing for MMF links have received considerable attention, and the utility of such techniques to increase data rates was first demonstrated by Stuart [3]. Optical MIMO techniques have been studied with both coherent [9] as well as in non-coherent [4] detection. In addition, mode-group diversity multiplexing for fiber links has been used as a multiplexing method for improving data rates within dispersion limits [6]. The feasibility of higher numbers of lasers and detectors being used to improve data rate performance was analyzed in [5], where a power diffusion approach was utilized to quantify the effectiveness of sending multiple parallel streams of data through the fiber using mode groups. However, the effect of device placement on the data rates was not discussed. Here, we utilize a field propagation analysis technique [8], in which we optimize laser and detector placements to maximize the (information theoretic) capacity MIMO-MMF links. These placements enable us to develop placement plural guidelines for designing feasible device arrays that work well in MMFs with MIMO and signal processing.

We develop a model that evaluates the MMF channel capacity for any laser and detector configuration butt-coupled to the MMF facets. This model uses a statistical description of the fiber that generates channel realizations. The (ergodic) capacity of each configuration is defined in the Shannon-theoretic sense as one averaged over a large number of realizations. We divide the space of all possible device positions into a grid and determine the configuration that yields the largest ergodic capacity.

The paper is organized as follows: Section II describes the physical model of the fiber channel and its statistical nature. Section III outlines the formulation of a MIMO system matrix for each channel realization, develops the input-output model, and discusses the metrics for determining the quality of the channel for given device configurations. Section IV describes the simulation of select configurations and shows that a best

configuration can be found under certain constraints. Finally, Section V concludes the paper.

II. Multimode Fiber Model

In order to model signal propagation through an MMF, we utilize tools developed by Shemirani et al. [8] to arrive at MIMO and signal processing metrics which can be optimized. We make use of this framework since it uses an electric field propagation based approach that results in a matrix model describing the input-output characteristics of a multimode fiber. Using this, we are able to predict experimentally observed phenomena with reasonable accuracy. Another model that could potentially be used is the diffusion power flow approach which treats modal coupling as a continuous power diffusion equation along the length of the fiber [10]. This diffusion model assumes that coupling occurs between nearest neighbor modes and accounts for a power loss mechanism with a mode-dependent parameter that is found experimentally [11]. While this approach [10] is suitable for modeling modal coupling, it does not take into account the polarization of the electric field and changes to its polarization by fiber non-idealities. As opposed to the diffusion-based approach, the technique developed by Shemirani et al. [8] treats modal coupling in a perturbation framework where the perturbing effect is due to bending and twisting of the fiber.

A. Propagation Matrix

The modes of an optical fiber form a spanning set for the solution of the Helmholtz wave equation. These eigenmodes are the well-established Hermite-Gauss functions [12]. Thus, we can decompose an electric field distribution guided by the fiber into a linear combination of these eigenmodes with complex coefficients. With this basis in mind, we form a vector that fully describes the electric field profile in the cross-section of the fiber. This vector can be found from the projection of an incoming electric field profile at the input facet of the optical fiber onto each of the fiber eigenmodes. This projection operation is given by the overlap integral of the incoming field and the eigenmodes.

To find the mode vector for a particular device, we make the assumption that the device electric field is a circularly symmetric Gaussian beam (TEM_{00} mode), and the size of the beam reflects the effective area of the device. The vector of modes each device couples to in the waveguide is evaluated by performing the overlap integral with the guided modes of the fiber. Let $E_L(x, y)$ be the incoming electric field due to a laser source polarized in the x-y plane, where the subscript L denotes a laser. Also, let $E_{(\tilde{p}\tilde{q})_F}(x, y)$ be the electric field distribution of the fiber eigenmode indexed by mode numbers $(\tilde{p}, \tilde{q})$ and polarized in the x-y plane. Then the complex entries of the vector corresponding to the incoming electric field are found by [12]

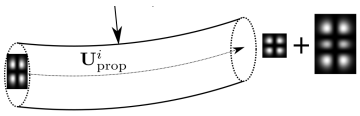

Fig. 1. $\mathbf{U}^i_{\text{prop}}$ describes intermodal coupling within a section

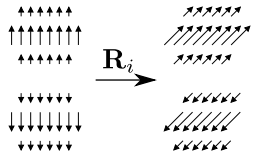

Fig. 2. $\mathbf{R}^i$ describes rotation of the polarization of the electric field at section junctions

$$a_{\tilde{p}\tilde{q}} = \frac{\langle E_L, E_{(\tilde{p}\tilde{q})_F} \rangle}{\sqrt{\langle E_L, E_L \rangle \langle E_{(\tilde{p}\tilde{q})_F}, E_{(\tilde{p}\tilde{q})_F} \rangle}} \tag{1}$$

$$\text{where } \langle A, B \rangle = \iint_{x,y} A(x, y) B^*(x, y) \, \mathrm{d}x \, \mathrm{d}y$$

Using the overlap integral, the input vector can be found as follows:

$$\underline{a}_L = \begin{bmatrix} \langle E_L, E_{F_1} \rangle \\ \langle E_L, E_{F_2} \rangle \\ \vdots \\ \langle E_L, E_{F_M} \rangle \end{bmatrix} \tag{2}$$

where $\underline{a}_L$ is an $M \times 1$ vector of complex numbers, with M being the number of modes propagating in the fiber. The number of modes supported by an optical fiber depends on the core diameter, wavelength of light, and the differences in refractive indices of the core and cladding. In particular, the number of modes increases with increasing core diameter. For instance, a weakly-guided multimode fiber with a diameter of 50 μm and nominal refractive index of 1.45 supports 55 guided modes. However, the electric field is polarized in the cross-section of the fiber and contains x and y components, each of which are represented by the guided modes of the fiber. In other words, the fiber possesses $55 \times 2 = 110$ modes. Thus, M defined here is twice the number of guided modes in the fiber and our model takes into account polarization induced birefringence.

Once an input vector is determined, a total propagation matrix $\mathbf{U}_{\text{total}}$ transforms the input electric field vector into the output electric field vector. The propagation matrix includes information about the power transfer between the eigenmodes and losses incurred during propagation from fiber perturbations. Decomposing the fiber into N small cascaded sections, propagation matrices can be found for the i-th section, $\mathbf{U}^i_{\text{section}}$. Multiplying these together yields the total propagation matrix $\mathbf{U}_{\text{total}} = \prod_{i=1}^{N} \mathbf{U}^i_{\text{section}}$.

The propagation matrix for the i-th section is a product of three matrices that account for three different effects. The

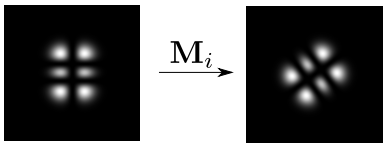

Fig. 3. $\mathbf{M}^i$ describes rotation of field profile due to fiber twists

first, $\mathbf{U}^i_{\text{prop}}$, contains the effects of intermodal coupling due to curvature of the fiber. As shown in Figure 1, a small curvature causes coupling of a mode into its nearest neighbor modes. This assumption is valid in situations where the bend radius r_i is large in comparison to the fiber core diameter. In Figure 2, a second matrix, $\mathbf{R}^i$, accounts for the rotation of the electric field vector at section junctions due to fiber twists. Finally, Figure 3 shows matrix $\mathbf{M}^i$ that accounts for mode profile rotations also due to fiber twists. The propagation matrix for the i-th section is then given by $\mathbf{U}^i_{\text{section}} = \prod_{i=1}^{N} \mathbf{M}^i \mathbf{R}^i \mathbf{U}^i_{\text{prop}}$.

To determine the response at the photodetector, an output vector $\underline{a}_D$ describing the coupling from the output facet to the photodetector is found using a technique similar to Equation 2. The inner product of this vector with the output field vector at the output facet of the optical fiber along with additive noise from the photodetector can be written conveniently in matrix notation as

$$y = \underline{a}_D^H \mathbf{U}_{\text{total}} \underline{a}_L + n \tag{3}$$

where $\mathbf{x}^H$ represents the conjugate transpose of $\mathbf{x}$ and n represents additive noise.

III. Analysis of System Matrix

In this section, we derive a MIMO system matrix model from the propagation framework for the MMF discussed in the previous section. We shall use this model to comment on how device placement can affect the performance of the link from a signal processing purview, analyze and design optimal laser and detector placement strategies which result in improved data rates through the MMF.

A. System Transfer Matrix

In order to arrive at a MIMO channel matrix, for each laser and detector in the configuration, an input vector describing its electric field profile is formed using the techniques of Section II-A. These are combined to obtain an effective channel matrix that reflects the MIMO input-output channel state from the transmitter to the receiver. Communication metrics, such as capacity, can be calculated with this MIMO matrix, which can be used to evaluate the effectiveness of a particular laser/detector configuration.

We assume that the matrix $\mathbf{U}_{\text{total}}$ describing the modal transformation induced by the MMF, while changing in time, changes sufficiently slowly, allowing us to estimate it and compensate for its effects. We shall discuss the implication of this on the optimization metric we consider in the subsequent section. This assumption is valid since the fiber channel is known to change slowly in comparison to the signaling rate [9, 13].

Using the overlap integral technique described in Equation 2, the input coupling vectors of each of the N_L lasers, represented as $\underline{a}_{L_1}, \underline{a}_{L_2}, \ldots \underline{a}_{L_{N_L}}$ can be found. Similarly, the output coupling vectors describing the overlap of different modes with each of the N_D detectors, represented by vectors $\underline{a}_{D_1}, \underline{a}_{D_2}, \ldots \underline{a}_{D_{N_D}}$ can be found. Since the overlap integral satisfies the properties of the inner product, the propagation of the initial vector induced by the array of lasers as well as the projection of the modes onto the array of detectors can be described with the matrix multiplication, as follows:

$$\mathbf{H}(t) = \mathbf{A}_D^H \mathbf{U}_{\text{total}}(t) \mathbf{A}_L \tag{4}$$

$$\mathbf{A}_L = \begin{bmatrix} | & | & \cdots & | \\ \underline{a}_{L_1} & \underline{a}_{L_2} & \cdots & \underline{a}_{L_{N_L}} \\ | & | & \cdots & | \end{bmatrix}$$

$$\mathbf{A}_D = \begin{bmatrix} | & | & \cdots & | \\ \underline{a}_{D_1} & \underline{a}_{D_2} & \cdots & \underline{a}_{D_{N_D}} \\ | & | & \cdots & | \end{bmatrix}$$

Here, $\mathbf{H}$ is an $N_D \times N_L$ matrix describing the channel state of the fiber channel, and $\mathbf{A}_L$ and $\mathbf{A}_D$ are, respectively, $M \times N_L$ and $M \times N_D$ matrices that describe the modal interaction of the lasers and detectors with the optical fiber. This framework allows the input-output relationship to be described in a compact fashion with input signals $x_1, x_2, \ldots x_{N_L}$, outputs $y_1, y_2, \ldots y_{N_D}$ and detector noise $n_1, n_2, \ldots n_{N_D}$ as

$$\begin{bmatrix} y_1(t) \\ y_2(t) \\ \vdots \\ y_{N_D}(t) \end{bmatrix} = \mathbf{H}(t) \begin{bmatrix} x_1(t) \\ x_2(t) \\ \vdots \\ x_{N_L}(t) \end{bmatrix} + \begin{bmatrix} n_1(t) \\ n_2(t) \\ \vdots \\ n_{N_D}(t) \end{bmatrix}. \tag{5}$$

In the equations above, the signals $x_i(t), 1 \le i \le N_L$ modulate the i-th laser, while the signals $y_j(t), 1 \le j \le N_D$ are received at the j-th photodetector. To analyze the performance of the MIMO system, it is assumed that the system is in the thermal noise limited regime, as opposed to being shot noise limited, which allows the additive noise to be modeled as white and Gaussian [9]. In addition, modal dispersion would cause pulse spreading due to differing phase velocities of different modes, but by using a modulation technique such as orthogonal frequency division multiplexing, the frequency selectivity due to pulse spreading can be converted to several smaller-bandwidth flat channels, thereby allowing dispersion-free modeling on a per-subchannel basis.

In the following subsection, we briefly describe the metrics we consider and the techniques we adopt to optimize for data rate performance.

B. Metrics for Optimization of Device Configurations

The primary metric of concern for optimizing the configurations of the laser and detector is the maximum achievable

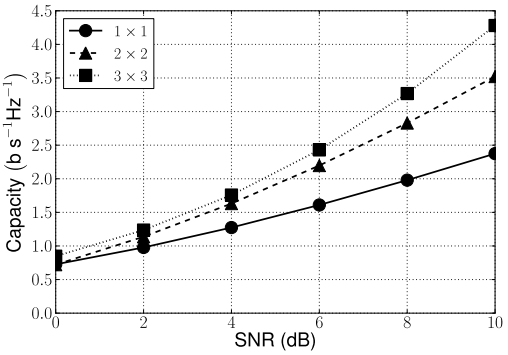

Fig. 4. Capacity vs. SNR for 1×1, 2×2, and 3×3 MIMO systems for the best device configuration

data rate through the fiber. For characterizing the potential data rate through the fiber, we consider the ergodic capacity of the fiber channel without channel state knowledge at transmitter, given by [7]

$$C = \mathbb{E}\left[\log\det\left(\mathbf{I}_{N_D} + \frac{\rho}{N_L}\mathbf{H}\mathbf{H}^H\right)\right] \tag{6}$$

where $\mathbf{I}_{N_D}$ is the $N_D \times N_D$ identity matrix and $\det$ represents the determinant operation.

Ergodic capacity is defined as the maximum rate that is obtainable through the fiber channel averaged over all realizations of the channel state for a transmission strategy which is based solely on the statistics of the channel, as opposed to a particular realization channel state itself. The utility of this metric in our optimization is that it accounts for the variations in the fiber channels with time, and thereby, ensures that the optimal array performs well under varying fiber channel conditions.

It must be noted that operating close to capacity would require the use of coherent detection. Intensity modulation provides for modulating only half of the laser waveform swing. The model that we consider accomadates the use of intensity modulation by restricting the data signals to be positive and real, and follows trends similar to those obtained with coherent detection. In addition, it is known that the capacity trends with increasing modulators and detectors shows a similar increasing trend to the coherent case at high SNR [7].

IV. Simulation Results

We performed a MATLAB-based simulation to determine the feasibility of optimizing a laser and detector configuration that yields the greatest ergodic capacity over the ensemble of channel realizations. From Section III, for a given configuration, the system matrix $\mathbf{H}$ is derived from $\mathbf{U}_{\text{total}}$. An ensemble of $\mathbf{U}_{\text{total}}$ corresponds to the ensemble of system realizations and thus, an ensemble of system matrices. We generate 700 realizations of $\mathbf{U}_{\text{total}}$ matrices. To find each $\mathbf{U}_{\text{total}}$, a graded-index fiber was split into 10,000 sections of 10 cm length each. The fiber has a diameter of 50 $\mu\mathrm{m}$, core index of refraction of 1.444 and a numerical aperture of 0.19. The lasers were assumed to operate at 1.55 $\mu\mathrm{m}$ in the fundamental mode, with an effective beam diameter of 12 $\mu\mathrm{m}$. A similar device configuration was used for the detectors. The electric field at the output of the fiber was assumed to couple into the fundamental detector mode. The statistical nature of the fiber comes from the curvature and twists in each section which are modeled by κ_i and θ_i respectively. Both are Gaussian random variables with κ_i having a standard deviation of .95 m^{-1}. The 10 cm fiber sections are sufficiently small in comparison to the radius of curvature of the sections to characterize modal propagation effects [8].

To simplify simulation in this initial study, the device configurations were restricted to rectangular 2-D arrays centered about the fiber axis. This assumption was chosen for convenience because it was shown to be feasible to fabricate [14]. A 3×3 grid was used both for the lasers and detectors. Our simulations demonstrate two ways of enhancing the capacity of the channel. First, it shows the effects on the data rate of an increasing number of transmitters and receivers. As expected, a larger number of devices can increase the data rate. Second, it shows that its possible to increase the capacity of a $N_L \times N_D$ MIMO system by fixing the laser and detector positions selectively on the grid.

To show the effect of an increasing number of devices on capacity, the 3×3 grid was fixed and each possible combination of laser and detector placements on this grid was considered. There are 9 possible grid positions, and if $N_L \neq 1$ lasers and $N_D \neq 1$ detectors are used, there are $\binom{9}{N_L} \times \binom{9}{N_D}$ device placements on this grid, and for each such combination, the average capacity over the 700 system matrices was found. If only one laser or detector was used, it was placed along the central axis of the fiber, since simulations for configurations with single devices on one side revealed that placing the device at the center provided the best capacity. For each $N_L \times N_D$ MIMO system, the combination of device placements on the grid was chosen to maximize the average capacity. The capacity vs. SNR for the best combination of a 1×1, 2×2, 3×3, system is shown in Figure 4. Compared with a 1×1 system at 10 dB SNR, the optimal 2×2 and 3×3 implementations yielded gains of 50% and 80% respectively. It is clear that when an increasing number of devices is used, the capacity improves greatly.

To show how the capacity of a $N_L \times N_D$ MIMO system can be increased with appropriate choice of laser and detector positions, the 3×3 grid is used for a 2×2 and 3×3 MIMO systems. The average capacity was found for each combination of the 2 (or 3) lasers and 2 (or 3) detectors on the grid. Figure 5 shows the capacity vs. SNR of a 2×2 MIMO system for the best combination, and compares it with a representative suboptimal combination. Figure 5(a) and 5(b) show the respective locations of the lasers and detectors for these combinations. It can be seen that if the best configuration is chosen at an SNR of 10 dB, the data rate can be increased to over 3 times the data rate of the suboptimal configuration. A similar analysis was performed for a 3×3 MIMO system,

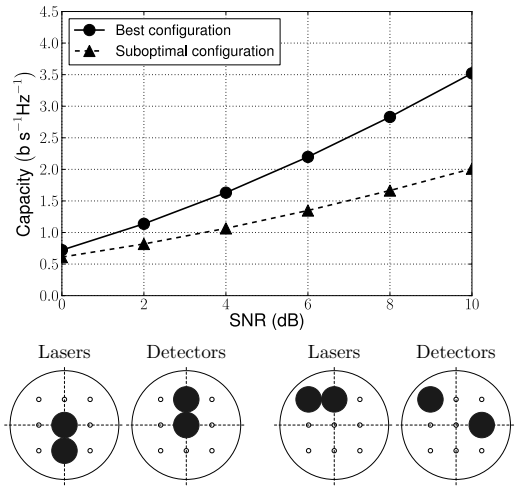

(a) Best Configuration (b) Suboptimal Configuration

Fig. 5. Capacity vs. SNR for a 2×2 MIMO system for the best device configuration and a suboptimal configuration in the plot above. The four circles at the bottom represent the fiber cross sections and the laser and detector placements on the cross sections that yielded both the best and suboptimal configurations. The small open white circles represent the grid points of allowed device positions and the large black circles represent the specific device placements associated with the configurations.

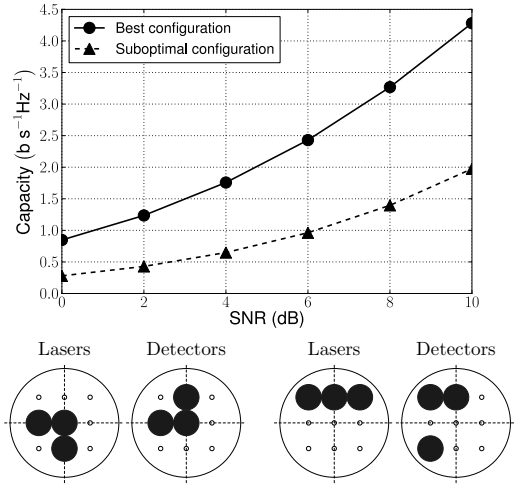

(a) Best Configuration (b) Suboptimal Configuration

Fig. 6. Capacity vs. SNR for a 3×3 MIMO system for the best device configuration and a suboptimal configuration in the plot above. The description of the subfigures is similar to that in Figure 5.

shown in Figure 6. In this case the data rate of the best configuration at an SNR of 10 dB is more than twice that of a suboptimal configuration. The above results of Figure 5 and 6 show that as opposed to a suboptimal configuration, the best configuration has a laser and detector placed at the center. This can be attributed to the prominence of the fundamental mode even at large distances. It is clear that the maximum achievable data rate can be significantly increased with appropriate configuration of the laser and detector arrays.

V. Conclusion

We have developed a statistical channel model for a MIMO system in a multimode fiber. Such an input-output signal processing model enables us to analyze the capacity of a multimode fiber link containing multiple lasers and detectors. In particular, we provide a means to analyze the link performance with particular geometries of laser and detector arrays, and demonstrate the importance in designing appropriate arrays of devices for maximum performance. With ergodic capacity as the design criteria, we numerically determined the optimal device arrays under appropriate feasibility constraints. These simulations revealed that systems with optimal device configurations could outperform arbitrarily chosen device arrays by $> 200\%$. Future work will involve evaluating the performance with finer grids, efficient search algorithms, and experimental verification.

References

[1] X. Shen, J. Kahn, and M. Horowitz, "Compensation for Multimode Fiber Dispersion by Adaptive Optics," *Optics letters*, vol. 30, no. 22, pp. 2985–2987, 2005.

[2] J. Peeters Weem, P. Kirkpatrick, and J. Verdiell, "Electronic Dispersion Compensation for 10 Gigabit Communication Links over FDDI Legacy Multimode Fiber," in *Optical Fiber Communication Conference*. Optical Society of America, 2005.

[3] H. R. Stuart, "Dispersive Multiplexing in Multimode Optical Fiber," *Science*, vol. 289, 2000.

[4] N. Bikhazi, M. Jensen, and A. Anderson, "MIMO Signaling over the MMF Optical Broadcast Channel with Square-law Detection," *Communications, IEEE Transactions on*, vol. 57, no. 3, pp. 614–617, 2009.

[5] M. Greenberg, M. Nazarathy, and M. Orenstein, "Data Parallelization by Optical MIMO Transmission over Multimode Fiber with Intermodal Coupling," *J. Lightw. Technol.*, vol. 25, no. 6, pp. 1503–1514, 2007.

[6] C. Tsekrekos, A. Martinez, F. Huijskens, and A. Koonen, "Mode Group Diversity Multiplexing Transceiver Design for Graded-Index Multimode Fibres," in *Optical Communication, 2005. ECOC 2005. 31st European Conference on*, vol. 3. IET, 2005, pp. 727–728.

[7] D. Tse and P. Viswanath, *Fundamentals of Wireless Communication*. Cambridge Univ Press, 2005.

[8] M. Shemirani, W. Mao, R. Panicker, and J. Kahn, "Principal Modes in Graded-Index Multimode Fiber in Presence of Spatial and Polarization-Mode Coupling," *J. Lightw. Technol.*, vol. 27, no. 10, pp. 1248–1261, 2009.

[9] A. R. Shah, R. C. J. Hsu, A. Tarighat, A. H. Sayed, and B. Jalali, "Coherent Optical MIMO (COMIMO)," *J. Lightw. Technol.*, vol. 23, 2005.

[10] G. Herskowitz, H. Kobrinski, and U. Levy, "Optical Power Distribution in Multimode Fibers with Angular-Dependent Mode Coupling," *J. Lightw. Technol.*, vol. 1, no. 4, pp. 548–554, 1983.

[11] D. Keck, "Spatial and Temporal Power Transfer Measurements on a Low-Loss Optical Waveguide," *Applied Optics*, vol. 13, no. 8, pp. 1882–1888, 1974.

[12] D. Marcuse, *Light Transmission Optics*. Van Nostrand Reinhold New York, 1982.

[13] C. Tsekrekos, M. de Boer, A. Martinez, F. Willems, and A. Koonen, "Temporal Stability of a Transparent Mode Group Diversity Multiplexing Link," *IEEE Photon. Technol. Lett.*, vol. 18, no. 23, pp. 2484–2486, 2006.

[14] E. Zeeb, B. Moller, C. Reiner, M. Ries, T. Hackbarth, and K. Ebeling, "Planar Proton implanted VCSEL's and Fiber-Coupled 2-D VCSEL Arrays," *Selected Topics in Quantum Electronics, IEEE Journal of*, vol. 1, no. 2, pp. 616–623, 1995.